Oncogene (2005) 24, 1150–1158

www.nature.com/onc

Cell cycle-dependent nucleocytoplasmic shuttling of the neurofibromatosis 2 tumour suppressor merlin

Taru Muranen*[,1,3], Mikaela Grönholm[1,3], G Herma Renkema[2] and Olli Carpén[1]

[1]*Program of Neuroscience, Biomedicum Helsinki, Department of Pathology, University of Helsinki and Helsinki University Hospital, PB 63, Helsinki 00014, Finland;* [2]*Institute of Medical Technology, University of Tampere and Tampere University Hospital, Finland*

The neurofibromatosis 2 tumour suppressor merlin/schwannomin is structurally related to the ezrin–radixin–moesin family of proteins, which anchor actin cytoskeleton to specific membrane proteins and participate in cell signalling. Merlin inhibits cell growth with a yet unknown mechanism. As most tumour suppressors are linked to cell cycle control, we investigated merlin's behaviour during cell cycle. In glioma and osteosarcoma cells, endogenous merlin was targeted to the nucleus in a cell cycle-specific manner. Merlin accumulated perinuclearly at the G2/M phase, and shifted to the nucleus at early G1. During mitosis, merlin localized to mitotic spindles and at the contractile ring. Nuclear merlin was strongly reduced in confluent cells. Blocking of the CRM1/exportin nuclear export pathway led to accumulation of merlin in the nucleus. Activation of the p21-activated kinase or protein kinase A, which result in phosphorylation of merlin, did not affect its nuclear localization. Merlin regulates the activity of extracellular signal-regulated kinase 2 (ERK2) and nuclear localization of both proteins was induced by cell adhesion. Unlike ERK2, nuclear localization of merlin was not, however, dependent on intact actin cytoskeleton. These results link merlin to events related to cell cycle control and may help to resolve its tumour suppressor function.
Oncogene (2005) **24,** 1150–1158. doi:10.1038/sj.onc.1208283
Published online 6 December 2004

Keywords: merlin; NF2; ERM; nucleus; cell cycle

Introduction

The neurofibromatosis 2 (*NF2*) gene is critically involved in the formation of tumours of the nervous system, especially schwannomas and meningiomas. In the NF2 disease, inherited *NF2* gene mutations result in multiple tumours, and in all sporadic schwannomas and most meningiomas somatic biallelic inactivation initiates tumour development (Baser *et al*., 2003). The mechanism by which the *NF2* gene product merlin (schwannomin) functions as a tumour suppressor is not known, although involvement in events related to cell cycle regulation has been suggested. For instance, overexpression of merlin in NIH3T3 cells reduces proliferation (Lutchman and Rouleau, 1995) and transfection of merlin into human primary schwannoma cells inhibits proliferation and promotes G0/G1 arrest (Schulze *et al*., 2002). Conversely, suppression of merlin in tumour cells induces proliferation (Huynh and Pulst, 1996) and targeted disruption of the *NF2* gene results in increased cell proliferation and tumour formation (McClatchey *et al*., 1998; Giovannini *et al*., 2000).

In general, functions of tumour suppressor proteins include regulation of cellular responses to growth-promoting signals, DNA damage and cell cycle checkpoints. These activities typically require nuclear localization of the tumour suppressor protein, which may occur in a cell cycle-specific manner. Regulated nucleocytoplasmic shuttling and association with the nuclear envelope and microtubules has recently been demonstrated for several tumour suppressor proteins, such as adenomatous polyposis coli (APC), VHL and BRCA1 (Fabbro and Henderson, 2003).

Merlin is structurally related to the ezrin, radixin and moesin (ERM-proteins), which act as molecular linkers between the cytoskeleton and specific membrane proteins (McClatchey, 2003). ERM-proteins are mainly found in actin-rich surface protrusions of the plasma membrane such as membrane ruffles, microspikes and in the cleavage furrow (Bretscher *et al*., 2002; Gautreau *et al*., 2002). Merlin partly colocalizes with ERM-proteins in these regions of dynamic cytoskeletal remodelling (Gonzalez-Agosti *et al*., 1996; Sainio *et al*., 1997; Shaw *et al*., 1998; Gusella *et al*., 1999) and forms heterodimers with ERM-proteins (Grönholm *et al*., 1999), especially when phosphorylated at S518 (Alfthan *et al*., 2004). Owing to this subcellular distribution, merlin has been regarded as a unique type of tumour suppressor, whose growth inhibitory mechanism would be linked to cell surface organization and adhesion. We show here, however, that the subcellular localization of merlin is more versatile than previously thought. Its nuclear localization is dependent on the cell cycle, cell density and adhesion.

*Correspondence: T Muranen; E-mail: taru.muranen@helsinki.fi
[3]These authors contributed equally to this work
Received 3 June 2004; revised 11 October 2004; accepted 12 October 2004; published online 6 December 2004

Results

Detection of nuclear merlin and its association with CRM1/exportin pathway

To study the localization of merlin, we used human U251 glioma and U2OS osteosarcoma tumour cell lines, expressing endogenous merlin. Under subconfluent conditions, and stained with three different merlin antibodies (Figure 1), merlin was concentrated underneath the cell membrane in line with earlier studies. However, a small fraction of cells demonstrated bright nuclear staining. The intensity of nuclear staining varied among cells, from cells exhibiting almost entirely nuclear labelling to cells with both nuclear and submembranous staining. In subconfluent cultures, the amount of cells demonstrating nuclear merlin varied (depending on the antibody) from 9 to 17% for U251 cells, and from 13 to 16% on U2OS cells. To verify the specificity of merlin antisera, 293HEK cells were transfected with myc-tagged merlin cDNA. Cells were then double-stained with myc mAb and merlin antisera (Figure 1c), or transfected protein was immunoprecipitated with myc mAb and the precipitated material was blotted with merlin antibodies (Figure 2c). Both immunostaining and co-immunoprecipitation results confirmed that the antibodies specifically recognise merlin.

We isolated the nuclear and cytoplasmic fractions and immunoblotted them for merlin, and for nuclear, membrane and cytoplasmic markers (Figure 2). Fractionation revealed the presence of merlin in the nuclear as well as in the membrane fraction and thus confirmed the immunolocalization results.

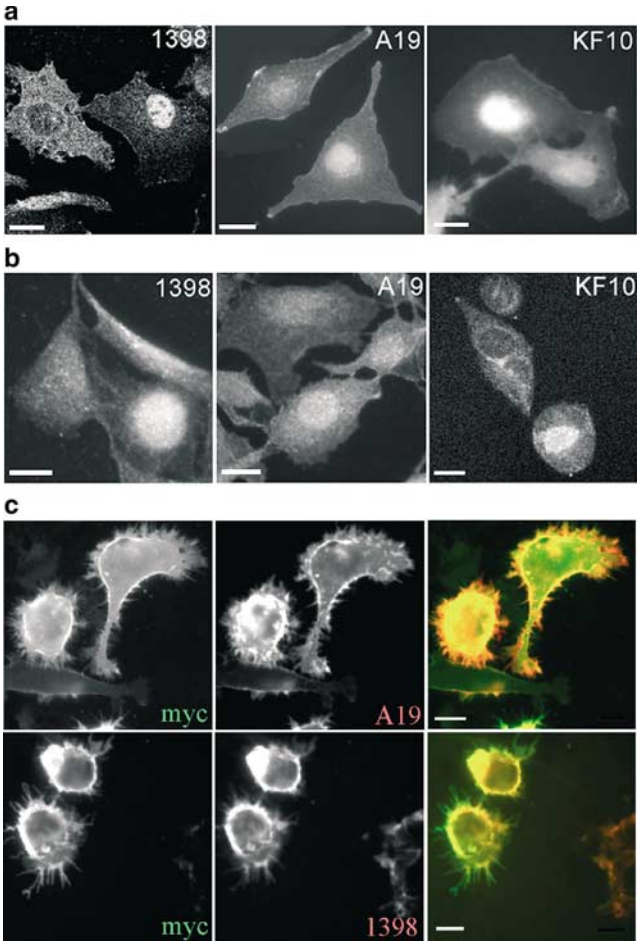

Figure 1 Endogenous merlin is present in the nuclei. (**a** and **b**) Immunostaining of subconfluent, nonsynchronized U251 glioma (**a**) and U2OS osteosarcoma cells (**b**) with three different merlin antibodies (1398, A19 and KF10) demonstrates nuclear staining in some cells. Subconfluent cultures were quantitatively analysed for nuclear merlin; 12% of U251 cells exhibit nuclear merlin (A19: 9.6%; 1398: 9.9%; KF10: 17%) and 14% of U2OS exhibit nuclear merlin (A19: 13.4%; 1398: 13.5%; KF10: 15.7%). The images were chosen to include cells with nuclear and the more frequent membrane/cytoplasmic staining pattern. To test the specificity of the polyclonal merlin antibodies, 293HEK cells were transfected with myc-tagged merlin cDNA (**c**). Cells were stained with myc mAb (green) and with polyclonal merlin antibodies, A19 and 1398 (red). Myc and merlin antibodies react with transfected cells only and demonstrate an identical staining pattern. Scale bar 10 μm

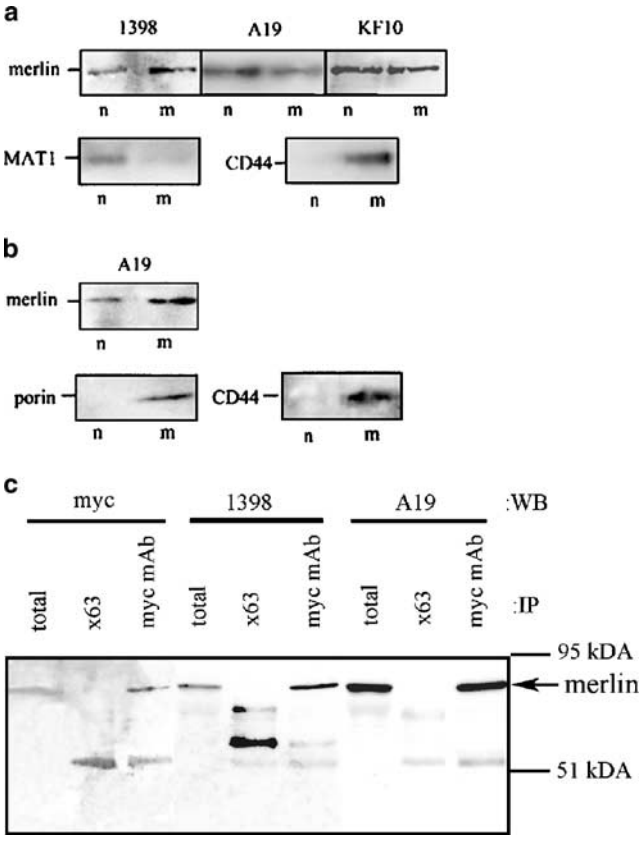

Figure 2 Subcellular fractionation of U251 and U2OS cells. (**a** and **b**) U251 (**a**) and U2OS (**b**) cells were fractionated and nuclear (n) and membrane/cytoplasmic (m) fractions were analysed by Western blotting. The three antibodies identify merlin both in the nuclear and in the membrane/cytoplasmic fractions. The nuclear marker MAT1 is detected predominantly in the nuclear fraction, and the transmembrane protein CD44 and the mitochondrial protein porin exclusively in the membrane/cytoplasmic fraction. The 293HEK cells were transfected with myc-tagged merlin cDNA (**c**). Transfected protein was immunoprecipitated with myc mAb or control X63 mAb and the precipitated material was blotted with polyclonal (A19, 1398) merlin antibodies or with myc mAb. All antibodies detect a band with the molecular size of merlin (arrow) in myc but not X63 mAb immunoprecipitates. The band is also detected in total lysates of transfected cells. The band above 51 kDa corresponds to antibody heavy chain

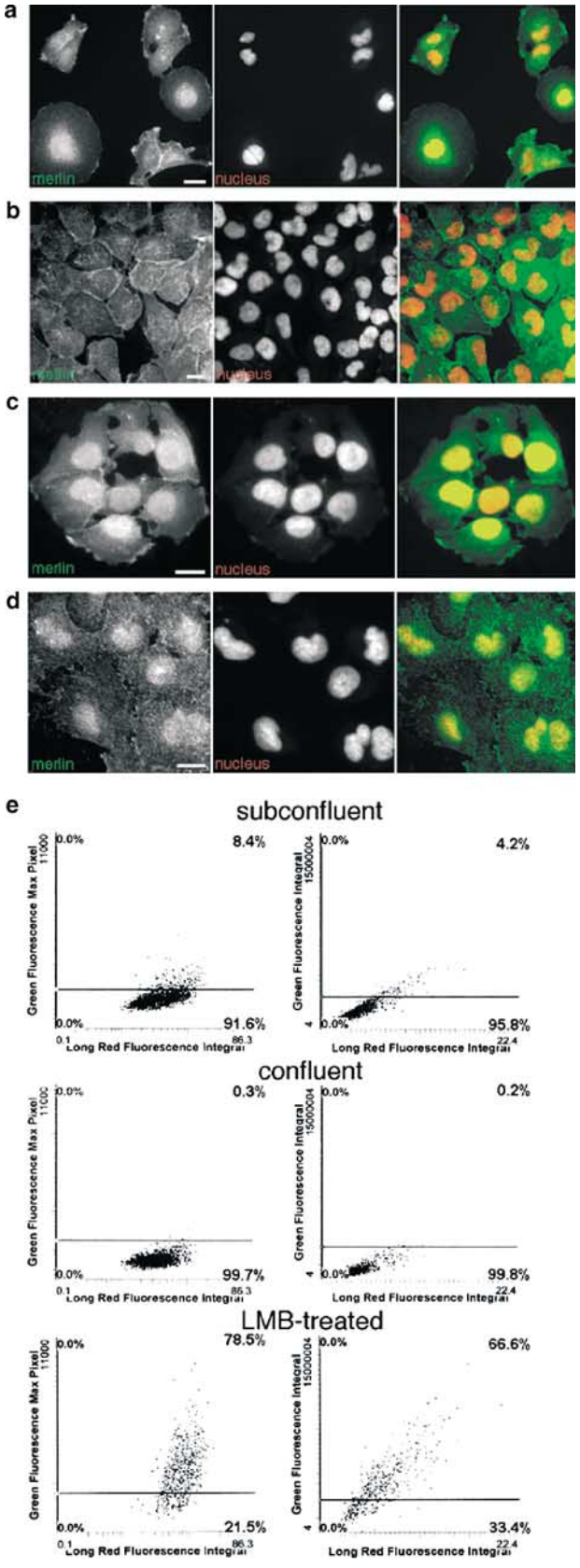

We next analysed whether cell density affects the distribution of merlin. Immunolocalization analysis of merlin demonstrated the presence of nuclear merlin in a fraction of cells grown in subconfluent conditions. Instead, in confluent cells, merlin was localized only to the cortical membrane and the cytoplasm, without a detectable nuclear signal (Figure 3). Laser scanning cytometric quantification of cells double-stained for merlin and DNA verified this finding (Figure 3).

Nucleocytoplasmic shuttling of proteins is an active process, regulated by various import and export pathways (Weis, 2003). To study the transport of merlin, we blocked the CRM1/exportin-mediated nuclear export with leptomycin B (LMB) (Kudo *et al*., 1998). LMB treatment of U251 cells resulted in a marked increase in nuclear merlin as demonstrated both by immunofluorescence microscopy and laser scanning cytometry (LSC) (Figure 3). After 2 h LMB treatment, most of the subconfluent cells demonstrated nuclear merlin and some nuclear accumulation was also seen in confluent cells. Nuclear localization was also evident in U2OS cells and the results for both cell lines were confirmed with all merlin antibodies (not shown).

Nuclear shuttling of merlin is linked to cell cycle

The differential nuclear localization of merlin in subconfluent cells suggested that nuclear targeting might occur in a cell cycle-specific manner. In order to study the localization of merlin in different phases of the cell cycle, subconfluent U251 cells were synchronized using nocodazole or mimosine treatment. Nocodazole depolymerizes microtubules reversibly and blocks cells at the G2/M phase, whereas mimosine affects the replication fork and blocks cells at early S phase. FACS analysis was used to confirm the efficiency of synchronization and to monitor the cell cycle phase after block release. In cells about to enter mitosis (late G2/M), merlin was localized in the cytoplasm and concentrated to the perinuclear region (Figure 4). During early mitosis, merlin was condensed around the breaking nuclear envelope, especially in nuclear envelope invaginations, that is, regions in which microtubules are concentrated

Figure 3 Cell confluency and LMB treatment affect nuclear localization of merlin (**a** and **d**). Subconfluent (**a**) or confluent (**b**) U251 cells were double-stained with merlin antibody (A19) and with a DNA-binding nuclear probe (TO-PRO). In contrast to subconfluent cells, in which nuclear merlin is detected, merlin in confluent cells is localized underneath the cortical membranes and in the cytoplasm and is absent from the nucleus. CRM1/exportin inhibitor LMB treatment of subconfluent cells results in nuclear accumulation of merlin (**c**). Increased nuclear staining is also detected in confluent cells after LMB treatment (**d**). Scale bar 10 μm. (**e**) LSC demonstrates quantitative differences in nuclear merlin content in subconfluent, confluent and LMB-treated cells. Propidium iodide staining (red fluorescence) was used to define the nuclear area and merlin staining (green) in the nuclei was quantified either as maximum pixel intensity (left) or total fluorescence in the nuclei (right). The percentage of cells with merlin-positive nuclei is shown in top right corner of each plot. This is a representative of three experiments

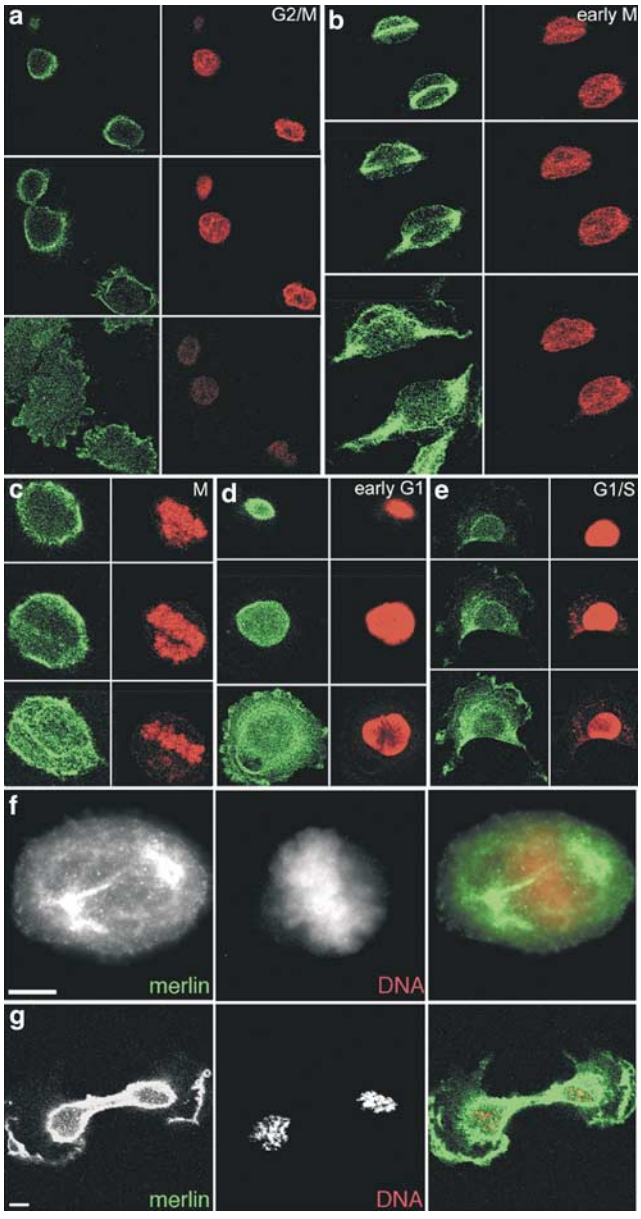

Figure 4 Subcellular localization of merlin is dependent on cell cycle. (**a–g**) U251 cells were synchronized with nocodazole and stained for merlin (NF2 1398 pAb, green) and DNA (TO-PRO, red) at various phases of the cell cycle and analysed by confocal microscopy. The cell cycle phase was verified by FACS analysis. Three different sections (dorsal, middle and ventral) are shown. The cells at the G2/M phase (**a**) (FACS analysis: G2/M 98.3%, G0/G1 1.5%, S 0.2%) show perinuclear accumulation of merlin. At early mitosis (**b**), merlin is concentrated around the breaking nuclear envelope, and the staining pattern is retained at the onset of mitosis (**c**). In early G1 (**d**), intense nuclear merlin staining is detected (FACS analysis: G2/M 71.9%, G0/G1 15.6%, S 12.5%). Later in the G1/S phase (FACS analysis: G2/M 14.0%, G0/G1 39.1% S 46.9%), merlin is absent from the nucleus and is concentrated underneath the cell membrane and in the cytoplasm (**e**). In mitotic cells, merlin staining coincides with mitotic spindles (**f**) and during cytokinesis merlin is seen around developing nuclear envelope and at mid-body (**g**). Scale bar 10 μm

in the prophase (Burke and Ellenberg, 2002). After mitosis, at early G1, merlin accumulated to the nucleus, and at this point a strong signal was also detected underneath the cortical membrane. Progression of the cell cycle to late G1 phase resulted in export of merlin from the nucleus. At G1/S, merlin concentrated underneath the cortical membrane and, less prominently, to the perinuclear region. Further analysis of merlin in dividing cells demonstrated a pattern resembling mitotic spindles in metaphase cells and concentration to the mid-body during cytokinesis (Figure 4).

Subcellular fractionation of synchronized U251 cells was performed to further analyse the distribution of merlin at different cell cycle phases. FACS analysis was used to confirm the synchronization (results not shown) and membrane and nuclear markers were used to verify the purity of subcellular fractions. Cells treated with mimosine and fractionated at block release (late G1/S) or 5 h later (S phase) showed only very little merlin in the nucleus, whereas the same treatment with nocodazole resulted in strong merlin reactivity in the nuclear fraction at the time of release (G2/M) and a weaker reactivity 5 h later (mid-G1) (Figure 5).

Phosphorylated merlin is present both in the nuclear and cytoplasmic fractions

Merlin has been shown to phosphorylate at serine 518 by p21-activated kinase (PAK) and protein kinase A (PKA) (Kissil *et al*., 2002; Xiao *et al*., 2002; Alfthan *et al*., 2004). The phosphorylated and nonphosphorylated forms of merlin can be identified by differential mobility in SDS–polyacrylamide gels (PAGE). As shown in Figure 5, both the hypophosphorylated and the phosphorylated forms of merlin were detected at all time points both in the nuclear and the cytoplasmic

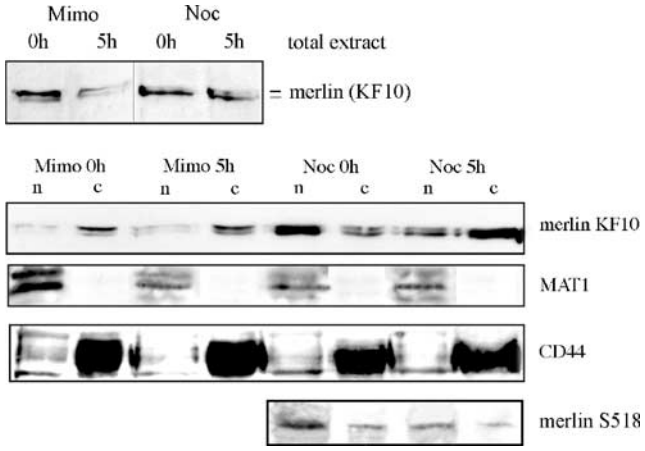

Figure 5 Merlin in subcellular fractions of synchronized cells. U251 cells were treated either with nocodazole (Noc), which blocks the cell cycle at G2/M or with mimosine (Mimo), which blocks the cell cycle at the beginning of the S phase, after which the block was released. Cells were fractionated immediately or 5 h after release of the block and nuclear (n) or membrane/cytoplasmic (m) fractions were analysed. Purity of the fractions was verified with a cytoplasmic marker CD44 and a nuclear marker MAT1. Merlin was detected with KF10 mAb and the S518 phosphorylated merlin was detected with S518-phospho-specific antibody. Also, total extracts of the synchronized cells are included. The cell cycle phase and synchronization was verified by FACS analysis (not shown)

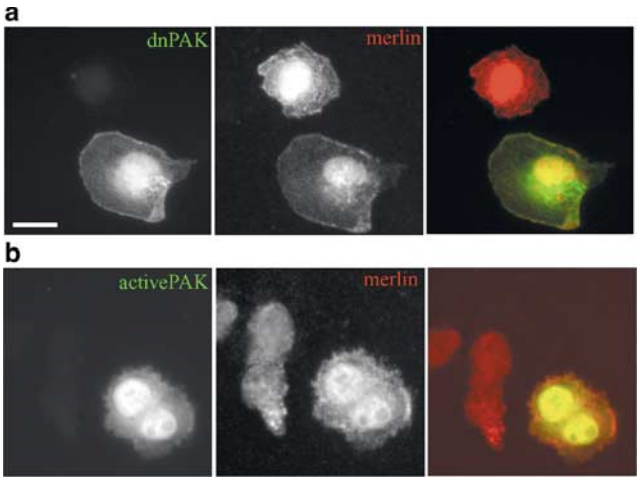

Figure 6 Regulation of PAK and PKA activity does not have a direct effect on merlin nuclear localization. U251 cells were transfected either with dominant-negative PAK2 construct (dnPAK) (**a**) or constitutively active PAK2 (active PAK) (**b**). dnPAK-expressing cells were incubated for 5 h with PKA inhibitor H89 before fixation. Cells expressing active PAK were incubated for 30 min with IBMX and forskolin before fixation. Merlin was detected with NF2 1398 antibody (red) and transfected cells with Myc mAb for dnPAK (green) or HA mAb for constitutively active PAK (green). Neither treatment has a direct effect on merlin nuclear localization. Scale bar 10 μm

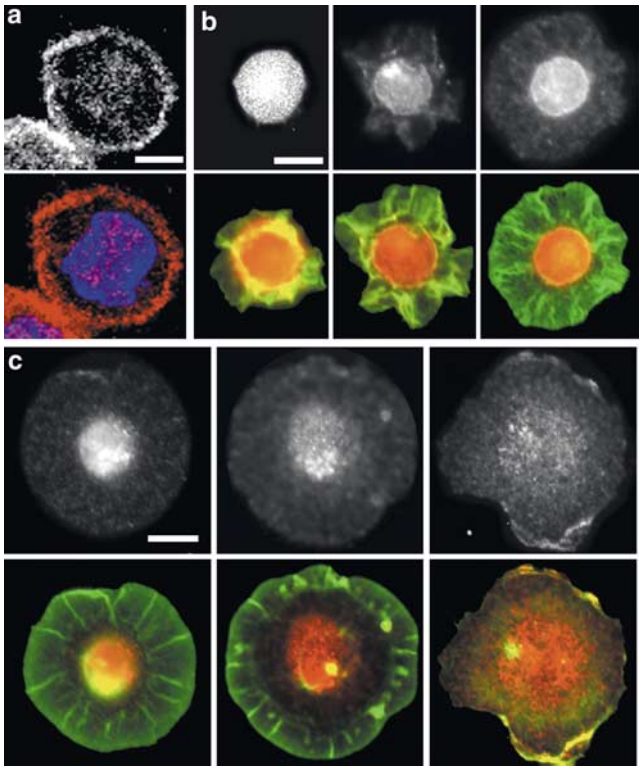

Figure 7 Merlin is targeted to the nuclei of attaching cells. U251 cells were trypsinized and fixed (**a**) or allowed to reattach on coverslips. Attaching cells were fixed after 30 (**b**) or 90 min (**c**). Merlin was stained with NF2 1398 Ab (red), nucleus with TO-PRO (blue) and F-actin was visualized with Oregon green phalloidin. Merlin is heavily accumulated in the nuclei during early phases of attachment. Scale bars, (**a**): 5 μm and (**b**, **c**) 10 μm

fraction. Further confirmation for the presence of phosphorylated merlin in both fractions was obtained by immunoblotting with an S518 phospho-specific merlin antibody (Figure 5).

We further studied whether alteration of the kinase activity changes the distribution of merlin at a cellular level. We transfected U251 cells with a dominant-negative PAK2 construct (inhibitory CRIB domain), known to inhibit endogenous PAK activity (Alfthan *et al*., 2004) and/or incubated the cells with H89, which blocks the PKA signalling pathway. This treatment has been shown to effectively block phosphorylation of merlin (Alfthan *et al*., 2004). In these cells, nuclear merlin staining was still evident (Figure 6). We also studied the effect of activation of PAK and PKA activity on the nuclear localization of merlin. U251 cells were transfected with constitutively active PAK2 construct and incubated for 30 min with IBMX and forskolin, which stimulate endogenous PKA activity in cells. This treatment did not induce any changes in the nuclear localization of merlin (Figure 6). The experiment was also performed with stimulated PKA together with inhibited PAK and *vice versa*. None of the treatments changed the nuclear localization of merlin.

Merlin is targeted to the nucleus at early phase of cell attachment

During mitosis, cells round up and are only loosely attached to the substratum. After cell division, they attach to substratum more firmly and spread again. We studied whether localization of merlin would be affected by cell attachment and spreading, which take place shortly after mitosis at G1. This was tested by either trypsinizing nonsynchronized, subconfluent U251 cells or, alternatively, by shaking off mitotic cells (not shown) and letting them reattach for a short time. Cells at various time points of reattachment were fixed and stained for merlin and F-actin. A strong nuclear merlin staining was detected at early phases of reattachment, both after mitotic shake off and trypsinization (Figure 7). At later time points (>1 h), when the cells were spread and the cortical lamellipodial actin network, typical of migrating cells, was formed, merlin was again concentrated underneath the membrane and nuclear localization disappeared (Figure 7).

Actin cytoskeleton is not required for adhesion-dependent nuclear targeting of merlin

Adhesion and cell spreading induce nuclear targeting of phosphorylated extracellular signal-regulated kinase (ERK) via a mechanism that requires intact actin cytoskeleton. Nuclear targeting of phosphorylated ERK is required for cell cycle progression at G1 (Aplin *et al*., 2001; Lohez *et al*., 2003). Merlin prolongs the G1 phase of the cell cycle (Schulze *et al*., 2002), possibly via inhibition of phosphorylation of ERK and ERK-

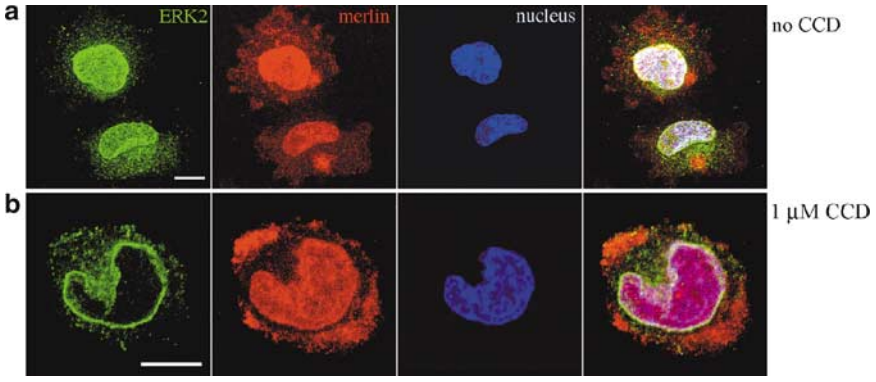

Figure 8 Nuclear localization of merlin is not dependent on intact actin cytoskeleton. U251 cells were serum starved, trypsinized and reattached on fibronectin-coated coverslips without serum and incubated without (**a**) or with CCD (**b**). Merlin was visualized with NF2 1398 Ab (red), ERK2 with mAb (green) and nuclei were detected with TO-PRO3 nuclear probe (blue). Confocal microscopic analysis of untreated cells demonstrates colocalization of merlin and ERK2 in the nuclei. In adhering cells, CCD treatment prevents nuclear targeting of ERK2, whereas merlin is still targeted to the nuclei. Scale bar 10 μm

dependent Elk-1 (Lim *et al*., 2003). We wanted to study whether merlin and ERK have similar requirements for adhesion-dependent nuclear localization, and whether they colocalize in cells with or without intact actin cytoskeleton. In untreated adhering cells, merlin colocalized with ERK2 in the nucleus (Figure 8). When adhering cells were either serum starved or grown in serum (not shown) and treated with cytochalasin D (CCD), which does not affect cell attachment but prevents cell spreading by disrupting the actin cytoskeleton, merlin still remained in the nucleus. Instead, ERK2 was concentrated outside the nuclear membrane in line with previous findings (Lohez *et al*., 2003), and no colocalization was seen between the two proteins (Figure 8). This result demonstrates that merlin's nuclear localization is not dependent on the nuclear localization of ERK, cell spreading nor an intact actin cytoskeleton. However, cell adhesion is required for the nuclear localization of merlin, since in nonadherent cells merlin is concentrated to the submembranous regions (Figure 7).

Discussion

Regulated movement between the nucleus and cytoplasm provides an efficient, simple and rapid way for tumour suppressors to control cell growth. Indeed, during recent years, many of the known tumour suppressors have been shown to undergo nucleocytoplasmic shuttling (Fabbro and Henderson, 2003). Although some studies, especially using transfected mutated merlin, have shown that it can be targeted to the nucleus and that its export is regulated by the CRM1 pathway (Kressel and Schmucker, 2002), merlin is generally regarded as a component of the cortical actin cytoskeleton. Therefore, its tumour suppressor mechanism has been considered unique. Merlin regulates cell growth by prolonging the G0/G1 phase of the cell cycle (Schulze *et al*., 2002), but it has not been evident as to how a submembranous protein could do this. Our current results provide a clue by demonstrating that endogenous merlin undergoes cell cycle- and anchorage-dependent nucleocytoplasmic shuttling in analogy with many other tumour suppressor proteins.

The amino-terminal part of merlin contains an FERM domain shared by several cytoskeletal molecules including band 4.1 proteins. Several isoforms of band 4.1 proteins are targeted to the nucleus by nuclear localization signals (NLS) that act in a hierarchical manner (Correas, 1991; De Carcer *et al*., 1995; Lallena and Correas, 1997). An important NLS in band 4.1 proteins is a stretch of basic residues (KKKR), which is suggested to bind to a negatively charged motif of importin (Gascard *et al*., 1999). Merlin contains an analogous stretch of basic residues ($_{309}$RRRK$_{312}$), which may be involved in its nuclear targeting. A further analogy between merlin and band 4.1 protein isoforms is their association with mitotic spindles during early mitosis (Krauss *et al*., 1997; Mattagajasingh *et al*., 1999). According to Kressel and Schmucker (2002), merlin exon 2 has a cytoplasmic retention signal, which keeps merlin in the cytoplasm. Thus, there may be several signal motifs with opposite effects, whose interplay dictates the cell cycle-dependent distribution of merlin. Unfortunately, our experiments with transiently transfected wild-type merlin have not been able to show a clear nuclear localization of the overexpressed as endogenous protein. For this reason, we have not tested how disruption of the potential NLS would affect its nuclear localization. We hypothesize that the lack of clear nuclear targeting of transfected protein is due to overexpression, but the reason for this dose dependency in subcellular localization remains to be studied further.

Time point assays with endogenous merlin imply that targeting to the nucleus is strictly controlled by cell cycle phase. Merlin is associated with mitotic spindles during mitosis (Muranen *et al*., in preparation) and is present in the nucleus at early G1 but not at late G1, S or G2 phase. The nuclear localization is seen in actively proliferating cells but not in cells influenced by

confluency or contact inhibition. A similar pattern of expression has also been shown for the APC and VHL tumour suppressors, which localize mostly in the cytoplasm of confluent cells and shift to the nucleus in subconfluent cells and affect growth in cell cycle-dependent manner (Lee *et al*., 1996; Zhang *et al*., 2001). The nucleocytoplasmic shuttling may also provide means for merlin to affect cell growth in the same manner.

Immunolocalization studies of adhering U251 cells, either after trypsination or mitotic shake off, indicate that merlin accumulates to the nucleus at early points of cell attachment. Adhesion and anchorage to the substratum are known to regulate cell cycle progression at early G1 (Assoian and Zhu, 1997). One of the key molecules is ERK, whose activity depends on integrin-mediated cell adhesion and the presence of an intact actin cytoskeleton. Phosphorylation of ERK and its translocation from the cytoplasm to the nucleus is required for cell cycle progression at G1. A downstream target of ERK in the nucleus is the Elk-1 transcription factor. Phosphorylated Elk-1 has increased affinity to the serum response element and enhances transcription of growth-related proteins (Marais *et al*., 1993; Whitmarsh *et al*., 1995; Vanhoutte *et al*., 2001), ultimately leading to the induction of a cell cycle protein cyclin D1 which regulates the passage through G1. Both merlin and ERK are localized in the nucleus of adhering cells and at early G1 phase of the cell cycle. This is of interest in light of a recent study that showed that merlin inhibits phosphorylation of ERK as well as ERK-dependent nuclear Elk-1 phosphorylation (Lim *et al*., 2003). However, in CCD-treated cells in which Elk-1 phosphorylation is impaired and ERK is unable to localize to the nucleus (Aplin *et al*., 2001), merlin is still found in the nucleus. This implies that merlin and ERK are targeted to the nucleus via different pathways and that nuclear localization of merlin does not depend on ERK's activity. There are two additional interesting molecular partners of merlin, paxillin and syntenin, whose nucleocytoplasmic shuttling has recently been demonstrated. Both of these molecules possess transcriptional potential (Aplin, 2003), and therefore their interaction with merlin should be studied with a novel perspective. Furthermore, a very recent study demonstrated that human polyoma virus T-antigen, which is able to transform cells of neural origin, is in complex with merlin in the nucleus of malignant peripheral nerve sheat tumours (Shollar *et al*., 2004). Interestingly, the authors report the presence of merlin in a fraction of unsynchronized tumour cells in line with our findings.

The activity of merlin is regulated by phosphorylation. Two types of kinases, PAK-1/2 and PKA, have been shown to phosphorylate merlin (Kissil *et al*., 2002; Xiao *et al*., 2002; Alfthan *et al*., 2004). The activity of PAKs is strongly regulated by adhesion. Therefore, regulation of the nuclear localization of merlin by phosphorylation is a tempting possibility. However, we found phosphorylated merlin both in the nuclear and cytoplasmic fractions and did not find direct evidence that activation or inhibition of PAK and/or PKA would have an obvious effect on its nuclear localization. However, we cannot exclude the possibility that there would be an indirect link between PAK-dependent phosphorylation of merlin and its subcellular targeting.

In conclusion, our study identifies two cell cycle phases, mitosis and early G1 phase, with novel specific targeting of merlin. These observations indicate that merlin may share activities of other tumour suppressor proteins and may provide a novel basis for the understanding of the biological functions of merlin.

Materials and methods

Cell culture, transfections and antibodies

U2OS osteosarcoma cells were maintained in Dulbecco's modified Eagle's medium with 1% nonessential amino acids, supplemented with 15% foetal calf serum (FCS) (PromoCell, Heidelberg, Germany), and U251 glioma cells were maintained in Dulbecco's minimum essential medium, supplemented with 10% FCS. The 293HEK cells were maintained in RPMI medium supplemented with 10% FCS. Cells were fixed in 3.5% paraformaldehyde (pH 7.5). Cells were transfected with Fugene6 (Roche, Mannheim, Germany) reagent and incubated for 48 h before analysis. PKA was stimulated by IBMX (50 μM) and forskolin (25 μM) for 30 min and inhibited by 5 h incubation with H89 (20 μM) (all provided by Sigma, St Louis, USA). Constitutively active PAK (T402E mutant) and the inhibitory N-terminal PAK2 construct (PAK2 1-248 H82/85L) were used as described (Alfthan *et al*., 2004).

Anti-merlin polyclonal Ab A-19 sc-331 (Santa Cruz Biotechnology, Santa Cruz, CA, USA), 1398 NF2 (den Bakker *et al*., 1995), anti-schwannomin (Lutchman and Rouleau, 1995) and mAb KF10 (den Bakker *et al*., 1995) were used. HM2175 antiserum (Kissil *et al*., 2002), kindly provided by Dr J Kissil (Massachusetts Institute of Technology, Cambridge, MA, USA), was used to detect S518 phosphorylated merlin. Anti-MAT1 fl-309 (Santa Cruz Biotechnology) pAb and CD44 mAb Hermes-3 (Jalkanen *et al*., 1987) were used in Western blotting. TO-PRO3-iodide probe (Molecular Probes, Eugene, OR, USA) was used for DNA staining. Myc mAb (Covance Research Products Inc., Princeton, NJ, USA) was used to detect tagged N-terminal domain of PAK2 and HA mAb (Roche) to detect tagged constitutively active PAK2. Anti-α-tubulin mAb N356 (Amersham Pharmacia Biotech, Buckinghamshire, England) was used to detect tubulin and propidium iodide to stain the nuclei in LSC and FACS analysis. Anti-porin mAb (Molecular Probes) was used as a cytoplasmic marker. Rabbit ERK2 Ab (Santa Cruz Biotechnology) was used to detect ERK2 and Oregon green- and rhodamine phalloidin (Molecular Probes) were used to detect F-actin. X63 mAb (ATCC) was used as a negative control. Alexa-488-, Alexa-568- and Alexa-594-conjugated goat anti-mouse and goat anti-rabbit antibodies (Molecular Probes) were used as secondary antibodies in immunofluorescence and HRP-conjugated rabbit anti-mouse and swine anti-rabbit secondary antibodies (DAKO A/S, Glostrup, Denmark) in Western blot analysis.

Subcellular fractionation and co-immunoprecipitation

Nuclear extract kit (Active Motif, Rixensart, Belgium) was used for nuclear and cytoplasmic fractionation. Protein concentration in each fraction was measured with Bradford

A595 assay and equal amounts of protein were loaded. For immunoblotting, proteins were separated on 8% SDS–PAGE, transferred to nitrocellulose membranes (Schleicher & Schuell, Dassel, Germany) and immunoblotted proteins were detected by enhanced chemiluminescence (Amersham Pharmacia Biotech). The 293HEK cells were transfected with myc-tagged merlin cDNA in pcDNA3 vector. After 48 h, the cells were lysed in ELB-NP40 buffer. Immunoprecipitations were performed by adding 6 μg of myc or X63 mAb to 300 μg of cell lysate. Lysates were incubated with the antibodies for 1 h at $+4^{\circ}$C before the addition of 30 μl of Protein G–Sepharose beads (Amersham Pharmacia Biotech), after which incubation was continued overnight at 4°C. Beads were precipitated by centrifugation (500 r.p.m., 5 min) and washed three times (ELB). Beads were eluted in 30 μl of 2 × reducing Laemmli buffer at 95°C. A measure of 15 μl of reactions was run on SDS–PAGE (8%).

Cell cycle synchronization and treatments

For cell cycle synchronization, U251 and U2OS cells were treated with nocodazole (200–400 ng/ml, Calbiochem, San Diego, CA, USA) or L-mimosine (200–400 μM, Calbiochem). After 18–24 h, the block was released. At various time points after release, samples were taken for FACS analysis, immunofluorescence and laser scanning confocal microscopy. Cells were not grown to confluency during the experiments. Cells for the CRM1-dependent nuclear export inhibition experiment were treated with LMB 5 ng/ml (Sigma) for 2 h. Cells from one 10 cm plate were lysed at each time point in ELB-NP40 buffer (150 mM NaCl, 50 mM HEPES (pH 7.4), 5 mM EDTA, 0.5% NP40, 1 mM EDTA, 10 mM $Na_4P_2O_7$, 50 mM NaF, 1 mM orthovanadate, 1.5 μM ocadaic acid and protease inhibitors, 0.5% NP40) and centrifuged for 30 min at 20 000 *g*. Protein amounts from each supernatant were equalized and analysed by Western blotting. A measure of 5 ml of PBS was swirled over subconfluent 10 cm plates and the plates were shaken heavily to detach mitotic cells. Cells were collected and run onto cytocentrifuge slides (700 r.p.m., 5 min). For disruption of the cytoskeleton, cells were serum starved for 24 h, trypsinized and reattached for 2 h on fibronectin-coated coverslips either with or without 10% FCS and with 1 μM CCD (Sigma).

Immunofluorescence and laser scanning confocal microscopy

Fixed cells were permeabilized in 0.1% Triton X-100/PBS and stained with merlin and tubulin antibodies followed by secondary antibodies. Coverslips were mounted in DABCO (Sigma) and Mowiol (Calbiochem) and examined by confocal microscopy (Leica SP2 equipped with Ar and Kr lasers, Leica Microsystems, Heerbrugg, Switzerland) using the sequential scanning mode or by immunofluorescence microscopy (Zeiss Axiophot equipped with AxioCam cooled CCD camera, Carl Zeiss, Esslingen, Germany). For analysis of cells with nuclear merlin staining, 400–600 cells per antibody were calculated.

Flow and LSC

Flow cytometric analysis was performed with a FACS Calibur (Beckton-Dickinson, San Jose, CA, USA). Cells from one 10 cm plate were trypsinized, washed in PBS twice, resuspended and fixed in 70% ethanol. Cells were dyed with propidium iodide for 15 min at $+37^{\circ}$C, after which the DNA amount was measured and analysed. For LSC, cells were stained with merlin antibody A19 followed by Alexa-488-conjugated secondary antibody and with propidium iodide (25 μg/ml in 50% glycerol) and analysed with a laser scanning cytometer (CompuCyte Corp., Cambridge, MA, USA) using argon ion laser excitation at 488 nm. Fluorescence was collected by photomultiplier tubes with green (530 DF 30) and red (600 DF 60) bandpass filters and digitized to 0.25 μm × 0.5 μm pixel resolution. The nuclei were identified by propidium iodide positivity and merlin staining in the nuclei calculated (total fluorescence and maximal pixel fluorescence). A total of 500–2000 cells per sample were analysed.

Abbreviations

APC, adenomatous polyposis coli; CCD, cytochalasin D; ERK2, extracellular signal-regulated kinase 2; ERM, ezrin–radixin–moesin; LMB, leptomycin B; LSC, laser scanning cytometry; NF2, neurofibromatosis 2.

Acknowledgements

We thank Dr Ellen Zwarthoff for generously providing the 1398 and KF10 antibodies, Dr Joseph Kissil for providing the HM2175 antibody, Hanne Ahola, Helena Ahola, Tuula Halmesvaara and Monica Schoultz for skillful technical assistance and Kaija Alfthan, Leena Heiska, Mikko Rönty and Anu Wartiovaara for fruitful discussions and assistance. This work was supported by the US Army Neurofibromatosis Research Grant DAMD17-00-0550 and the Academy of Finland.

References

Alfthan K, Heiska L, Grönholm M, Renkema H and Carpén O. (2004). *J. Biol. Chem.*, **279,** 18559–18566.
Aplin AE. (2003). *FEBS Lett.*, **534,** 11–14.
Aplin AE, Stewart SA, Assoian RK and Juliano RL. (2001). *J. Cell Biol.*, **153,** 273–281.
Assoian RK and Zhu X. (1997). *Curr. Opin. Cell Biol.*, **9,** 93–98.
Baser ME, Evans RDG and Gutmann DH. (2003). *Curr. Opin. Neurol.*, **16,** 27–33.
Bretscher A, Edwards K and Fehon RG. (2002). *Nat. Rev. Mol. Cell. Biol.*, **3,** 586–599.
Burke B and Ellenberg J. (2002). *Nat. Rev. Mol. Cell. Biol.*, **3,** 487–497.
Correas I. (1991). *Biochem. J.*, **279,** 581–585.
De Carcer G, Lallena MJ and Correas I. (1995). *Biochem. J.*, **312,** 871–877.
den Bakker MA, Riegman PH, Hekman RA, Boersma W, Janssen PJ, van der Kwast TH and Zwarthoff EC. (1995). *Oncogene*, **10,** 757–763.
Fabbro M and Henderson BR. (2003). *Exp. Cell Res.*, **282,** 59–69.
Gascard P, Nunomura W, Lee G, Walensky LD, Krauss SW, Takakuwa Y, Chasis JA, Mohandas N and Conboy JG. (1999). *Mol. Cell. Biol.*, **10,** 1783–1798.
Gautreau A, Louvard D and Arpin M. (2002). *Curr. Opin. Cell Biol.*, **14,** 104–109.
Giovannini M, Robanus-Maandag E, van der Valk M, Niwa-Kawakita M, Abramowski V, Goutebroze L, Woodruff JM, Berns A and Thomas G. (2000). *Genes Dev.*, **14,** 1617–1630.
Gonzalez-Agosti C, Xu L, Pinney D, Beauchamp R, Hobbs W, Gusella J and Ramesh V. (1996). *Oncogene*, **13,** 1239–1247.

Grönholm M, Sainio M, Zhao F, Heiska L, Vaheri A and Carpén O. (1999). *J. Cell Sci.*, **112,** 895–904.
Gusella JF, Ramesh V, MacCollin M and Jacoby LB. (1999). *Biochim. Biophys. Acta*, **1423,** M29–M36.
Huynh DP and Pulst SM. (1996). *Oncogene*, **13,** 73–84.
Jalkanen M, Rapraeger A, Saunders S and Bernfield M. (1987). *J. Cell Biol.*, **105,** 983–990.
Kissil JL, Johnson KC, Eckman MS and Jacks T. (2002). *J. Biol. Chem.*, **277,** 10394–10399.
Krauss SW, Larabell CA, Lockett S, Gascard P, Penman S, Mohandas N and Chasis JA. (1997). *J. Cell Biol.*, **137,** 275–289.
Kressel M and Schmucker B. (2002). *Hum. Mol. Genet.*, **11,** 2269–2278.
Kudo N, Wolff B, Sekimoto T, Schreiner EP, Yoneda Y, Yanagida M, Horinouchi S and Yoshida M. (1998). *Exp. Cell Res.*, **242,** 540–547.
Lallena MJ and Correas I. (1997). *J. Cell Sci.*, **110,** 239–247.
Lee S, Chen DYT, Humphrey JS, Gnarra JR, Linehan WM and Klausner RD. (1996). *Proc. Natl. Acad. Sci. USA*, **93,** 1770–1775.
Lim JY, Kim H, Kim YH, Kim SW, Huh PW, Lee KH, Jeun SS, Rha HK and Kang JK. (2003). *Biochem. Biophys. Res. Commun.*, **302,** 238–245.
Lohez OD, Reynaud C, Borel F, Andreassen PR and Margolis RL. (2003). *J. Cell Biol.*, **161,** 67–77.
Lutchman M and Rouleau GA. (1995). *Cancer Res.*, **55,** 2270–2274.
Marais R, Wynne J and Treisman R. (1993). *Cell*, **73,** 381–393.
Mattagajasingh SN, Huang SC, Hartenstein JS, Snyder M, Marchesi VT and Benz EJ. (1999). *J. Cell Biol.*, **145,** 29–43.
McClatchey AI. (2003). *Nat. Rev. Cancer*, **3,** 877–883.
McClatchey AI, Saotome I, Mercer K, Crowley D, Gusella JF, Bronson RT and Jacks T. (1998). *Genes Dev.*, **12,** 1121–1133.
Sainio M, Zhao F, Heiska L, Turunen O, den Bakker M, Zwarthoff E, Lutchman M, Rouleau GA, Jaaskelainen J, Vaheri A and Carpen O. (1997). *J. Cell Sci.*, **110,** 2249–2260.
Schulze KM, Hanemann CO, Muller HW and Hanenberg H. (2002). *Hum. Mol. Genet.*, **11,** 69–76.
Shaw RJ, McClatchey AI and Jacks T. (1998). *Cell Growth Differ.*, **9,** 287–296.
Shollar D, Del Valle L, Khalili K, Otte J and Gordon J. (2004). *Oncogene*, **23,** 5459–5467.
Vanhoutte P, Nissen JL, Brugg B, Gaspera BD, Besson MJ, Hipskind RA and Caboche J. (2001). *J. Biol. Chem.*, **276,** 5189–5196.
Weis K. (2003). *Cell*, **112,** 441–451.
Whitmarsh AJ, Shore P, Sharrocks AD and Davis RJ. (1995). *Science*, **269,** 403–407.
Xiao GH, Beeser A, Chernoff J and Testa JR. (2002). *J. Biol. Chem.*, **277,** 883–886.
Zhang F, White RL and Neufeld KL. (2001). *Mol. Cell. Biol.*, **21,** 8143–8156.